REGULAR ARTICLE

blood advances

The characteristics of vessel lining cells in normal spleens and their role in the pathobiology of myelofibrosis

Jiajing Qiu,[1] Mohamed E. Salama,[2] Cing Siang Hu,[1] Yan Li,[1] Xiaoli Wang,[1] and Ronald Hoffman[1]

[1]Division of Hematology/Medical Oncology, Department of Medicine, Tisch Cancer Institute, Icahn School of Medicine at Mount Sinai, New York, NY; and [2]Division of Hematopathology, Department of Pathology and Laboratory Medicine, Mayo Clinic, Rochester, MN

Key Points

- SVECs support the development of hematopoiesis in MF.
- LCs and SVECs each have distinct properties and functions that differ between normal and MF spleens.

The $CD34^{-}CD8\alpha^{+}$, sinusoid lining, littoral cells (LCs), and $CD34^{+}CD8\alpha^{-}$, splenic vascular endothelial cells (SVECs) represent 2 distinct cellular types that line the vessels within normal spleens and those of patients with myelofibrosis (MF). To further understand the respective roles of LCs and SVECs, each was purified from normal and MF spleens, cultured, and characterized. Gene expression profiling indicated that LCs were a specialized type of SVEC. LCs possessed a distinct gene expression profile associated with cytoskeleton regulation, cellular interactions, endocytosis, and iron transport. LCs also were characterized by strong phagocytic activity, less robust tube-forming capacity and a limited proliferative potential. These characteristics underlie the role of LCs as cellular filters and scavengers. Although normal LCs and SVECs produced overlapping as well as distinct hematopoietic factors and adhesion molecules, the gene expression profile of MF LCs and SVECs distinguished them from their normal counterparts. MF SVECs were characterized by activated interferon signaling and cell cycle progression pathways and increased vascular endothelial growth factor receptor, angiopoietin-2, stem cell factor, interleukin (IL)-33, Notch ligands, and IL-15 transcripts. In contrast, the transcription profile of MF LCs was associated with mitochondrial dysfunction, reduced energy production, protein biosynthesis, and catabolism. Normal SVECs formed in vitro confluent cell layers that supported MF hematopoietic colony formation to a greater extent than normal colony formation. These data provide an explanation for the reduced density of LCs observed within MF spleens and indicate the role of SVECs in the development of extramedullary hematopoiesis in MF.

Introduction

The splenic vasculature is composed of a complex network of capillaries, venules, arterioles, and sinuses. The littoral cells (LCs) that line the sinus walls serve as filters for altered or senescent red blood cells (RBCs)[1-4] and make up about 30% of the red pulp within the human spleen. Because the spleens of mice are asinusoidal, murine models that resemble the human spleen are not readily available. LCs have a distinct structure, phenotype, and function compared with other splenic vascular endothelial cells (SVECs) that line the splenic venules, capillaries, and arterioles.[1,2,5] LCs share the characteristics of both phagocytes and ECs. Although LCs express CD31 (PECAM1) and von Willebrand factor (VWF), they do not express the CD34 antigen.[6] LCs exclusively express $CD8\alpha/\alpha$, as well as scavenger receptors such as Stabilin-1 and the macrophage mannose receptor CD206.[7] LCs are, however, CD45-negative and do not express other T-cell markers including CD8β, CD4, or CD3. Furthermore, the cytoskeleton organizer FHOD1 is highly expressed by LCs, but not by

Submitted 7 December 2017; accepted 13 March 2018. DOI 10.1182/bloodadvances.2017015073.

The full-text version of this article contains a data supplement.

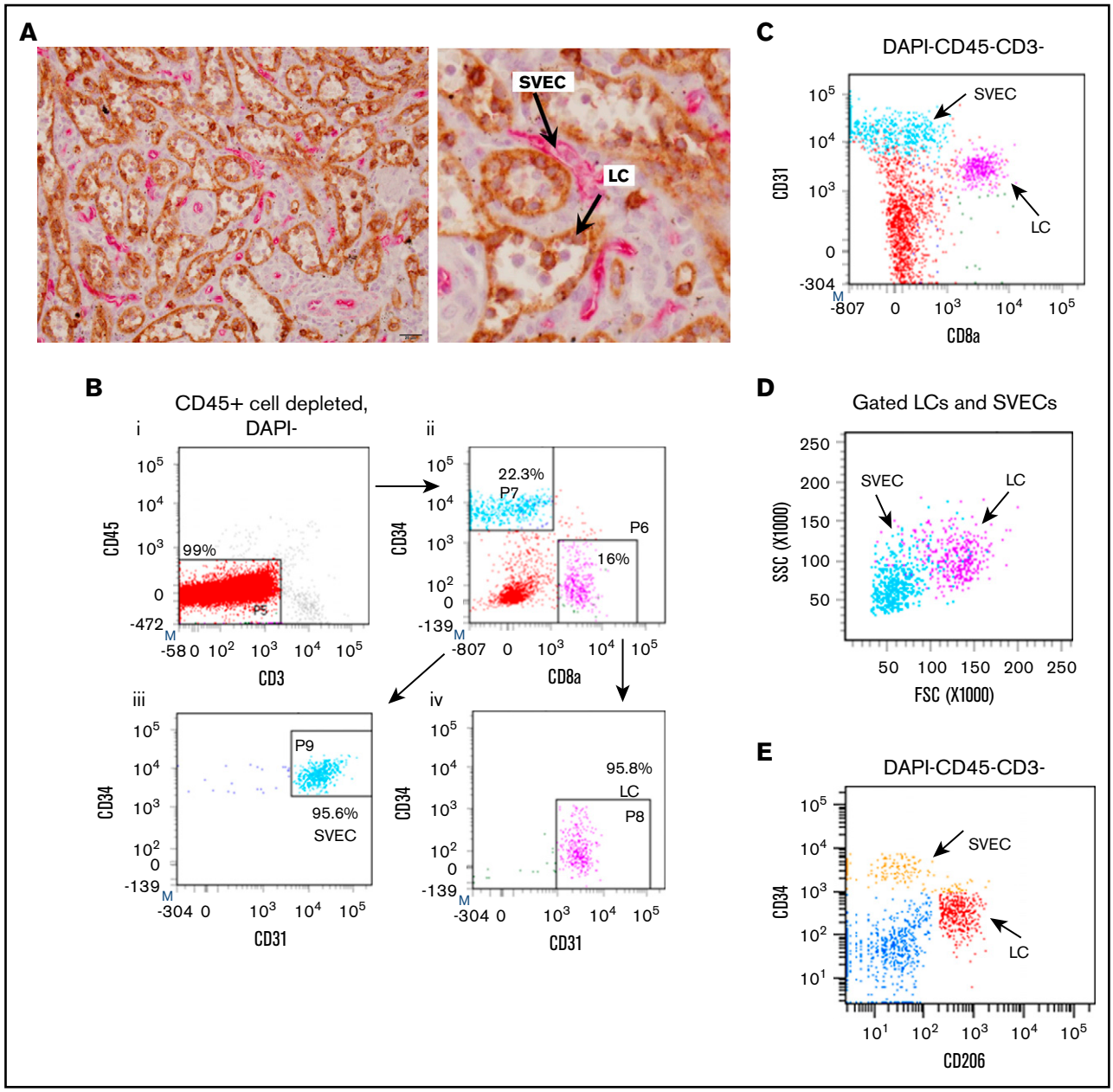

Figure 1. Isolation of viable LCs by FACS. (A) Representative photomicrograph of the red pulp of a normal spleen stained with both anti-CD8α (brown) and anti-CD34 (magenta) antibodies (original magnification ×400; scale bar, 20 μm). (Right) Enlarged image of a part of the left panel. Arrows show LCs (brown) and SVECs (magenta). (B) The gating strategy for sorting SVECs and LCs. $CD45^+$-cell depleted, $DAPI^-$ viable single cells of collagenase B digested spleen specimens were first gated for $CD45^-CD3^-$ population (i). More than 99% of the $CD45^+$ cell-depleted cells were $CD45^-CD3^-$. $CD45^-CD3^-$ cells were then gated for $CD34^+CD8\alpha^-$ or $CD34^-CD8\alpha^+$ populations (ii), which were then gated for $CD45^-CD3^-CD34^+CD8\alpha^-CD31^+$ SVECs (iii, light blue) and $CD45^-CD3^-CD34^-CD8\alpha^+CD31^+$ LCs (iv, magenta). Negative gates were determined according to corresponding isotype control staining. (C) CD31/CD8α FACS profiles of $DAPI^-CD45^-CD3^-$ cells. (D) SSC/FSC FACS profiles of back gated LCs (magenta) and SVECs (light blue) from panel B. (E) CD34/CD206 FACS profiles of $DAPI^-CD45^-CD3^-$ cells.

SVECs or other liver and bone marrow sinus lining cells.[7,8] Pinocytotic vesicles, lysosomes, phagocytosed RBCs, and cellular debris are often present within the cytoplasm of LCs reflective of their phagocytic capabilities.[1,7,9-12] Many of the prior observations concerning LCs have been made using electron microscopic and immunohistochemical staining, whereas the study of isolated purified cell populations has remained limited.

Although the human spleen is not normally a hematopoietic organ, spleens from patients with myelofibrosis (MF) are characterized by the development of extramedullary hematopoiesis (EMH). The vascular lining cells within MF spleens are thought to serve as a supportive microenvironment for MF hematopoietic cells.[13-16] Barosi and coworkers have reported that the capillary, but not sinusoidal, vascular density was increased within the MF spleen,[17]

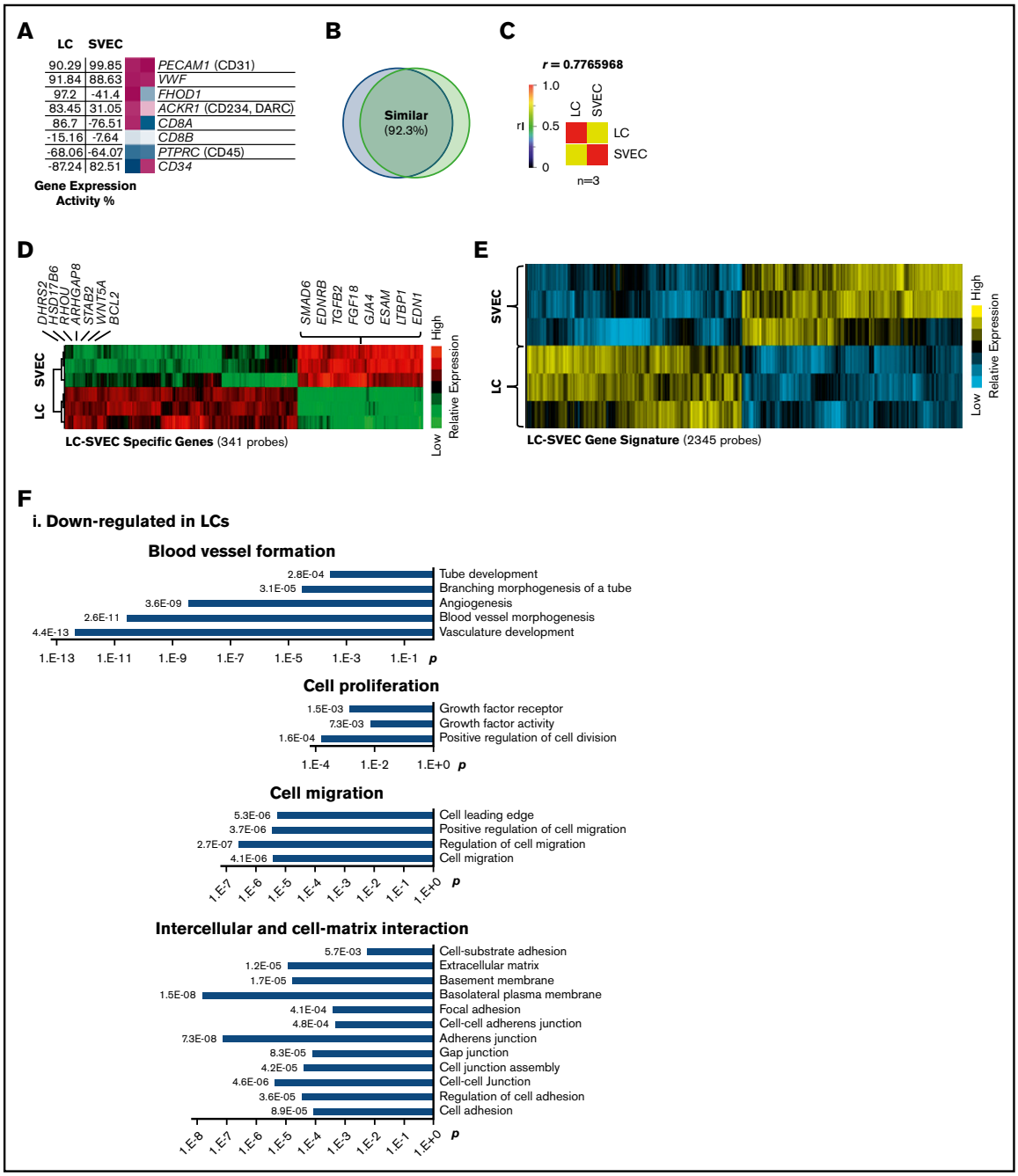

Figure 2. Global gene expression profiling of LCs and SVECs. (A) The GEA values and heat maps of selected genes obtained from GEXC analysis. The GEA values are listed in the data tables to the left of the heat maps. Magenta, high expression; white, threshold level expression; blue, low expression. GEA values are percentile ranks comparing the expression intensity in the data sets to the common reference of pooled human microarray data from various cell types and tissues (see supplemental Data for more information). (B) A diagram of the percentage of similarly expressed genes between LCs and SVECs. (C) Pearson correlation coefficient (*r*) by GEA between LCs and SVECs obtained from GEXC analysis. *r* value was calculated according to biological replicates of microarrays from 3 different normal spleen samples. (D) The heat map of relative expression intensity of LC-SVEC specific genes detected by 341 probes selected using stringent criteria. Selected downregulated genes and the top 20 upregulated genes are listed at the side. (E) The heat map of relative gene expression intensity for LC-SVEC gene signature containing differentially expressed genes detected by 2345 probes. (F) DAVID Functional Annotation Clustering of genes in LC-SVEC gene signature. Downregulated genes in LCs involving blood vessel formation, cell proliferation, and cell migration and intercellular and cell–extracellular matrix interaction (i); upregulated genes in LCs involving endocytosis, and intracellular transportation and iron transportation (ii); differentially expressed cell skeleton genes and genes in Rho GTPase signaling pathway (iii). (G,I) The GEA values (as described in Figure 2A) of genes involved in phagocytosis and genes encoding macrophage/monocyte antigens (G), and genes encoding Rho GTPase signaling pathway members (I). (H,J) RT-qPCR analysis of *TFRC* (transferrin receptor), *MRC1* (CD206), and *STAB2* (Stabilin-2) (H); *RHOU* (J). The expression of all genes was normalized to *GAPDH*, and the relative expression of a LC gene was calculated against that of SVEC, which was set as 1. Expression of housekeeping gene *HPRT* was included in each plot as a control. Data are shown as mean ± standard deviation (SD) of triplicate analyses.

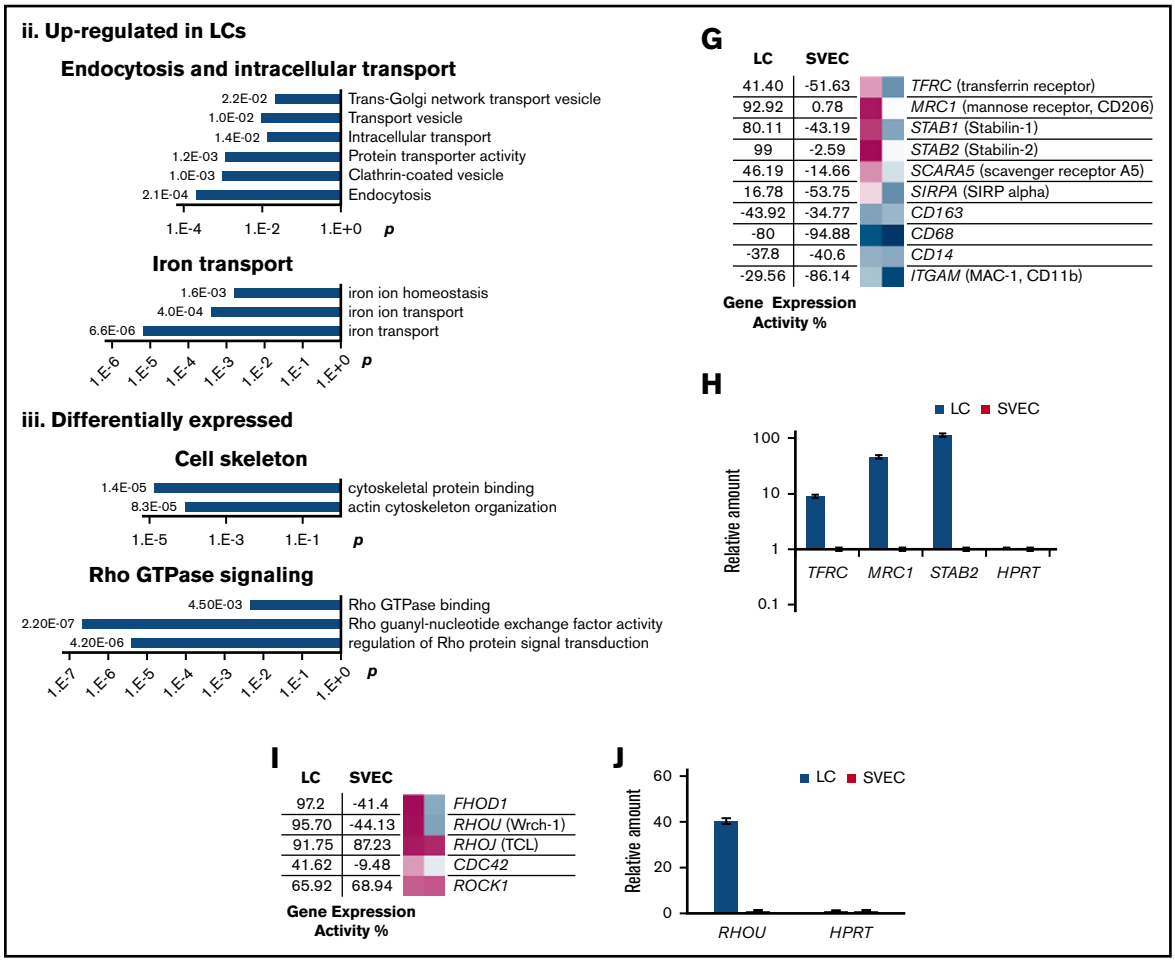

Figure 2. (Continued).

suggesting that the capillary lining SVECs and sinusoidal lining LCs may have distinct roles in the pathobiology of MF. In this report, we provide a detailed analysis of LCs and SVECs isolated from normal and MF spleens and report that these 2 cell populations have distinctive properties and contribute differently to the microenvironment of MF spleens.

Methods

Spleen specimen collection and cell preparation

Normal human spleens were obtained from the National Disease Research Interchange from healthy donors who required splenectomy after a traumatic injury. MF spleens were obtained from patients with advanced forms of MF who have marked splenomegaly and were undergoing therapeutic splenectomy after informed consent was obtained after approval by the Committee for Human Investigations at the Icahn School of Medicine at Mount Sinai. Additional information can be found in supplemental Methods.

Immunostaining, cell sorting, and antigen profiling of SVECs and LCs

$CD45^+$ cells were first magnetically depleted from collagenase B digested splenic single-cell suspension, using an anti-hCD45 depletion kit (StemCell Technologies), followed by staining with fluorochrome-conjugated monoclonal antibodies (mAbs) against CD45, CD3, CD34, CD8α, and CD31, and then the cell populations were sorted with a FACSArial II cell sorter (BD Biosciences). Immunostaining and fluorescence-activated cell sorter (FACS) analysis of additional antigens were performed using a FACS LSR Fortessa analyzer and analyzed with FACS Express 6 Flow Research software following standard procedures, which are detailed in supplemental Methods.

RNA isolation, amplification, and microarray analysis

Total RNA was individually extracted from viable LCs and SVECs isolated from normal and MF spleens by cell sorting and were amplified in vitro before being hybridized to Affymetrix human genome U133 Plus 2.0 arrays. Clustering was applied to the data sets, using Cluster 3.0 software.[18] Heat maps were generated with Java TreeView 3.0.[19] The microarray data are available through the Gene Expression Omnibus Series GSE106532. These studies were performed with spleens from 3 normal individuals and 3 patients with MF. More information is provided in the supplemental Methods.

LC and SVEC cultures

FACS-sorted LCs or SVECs were seeded onto fibronectin-coated[20] 96-well plates at 1×10^5 cells/well in endothelial cell medium

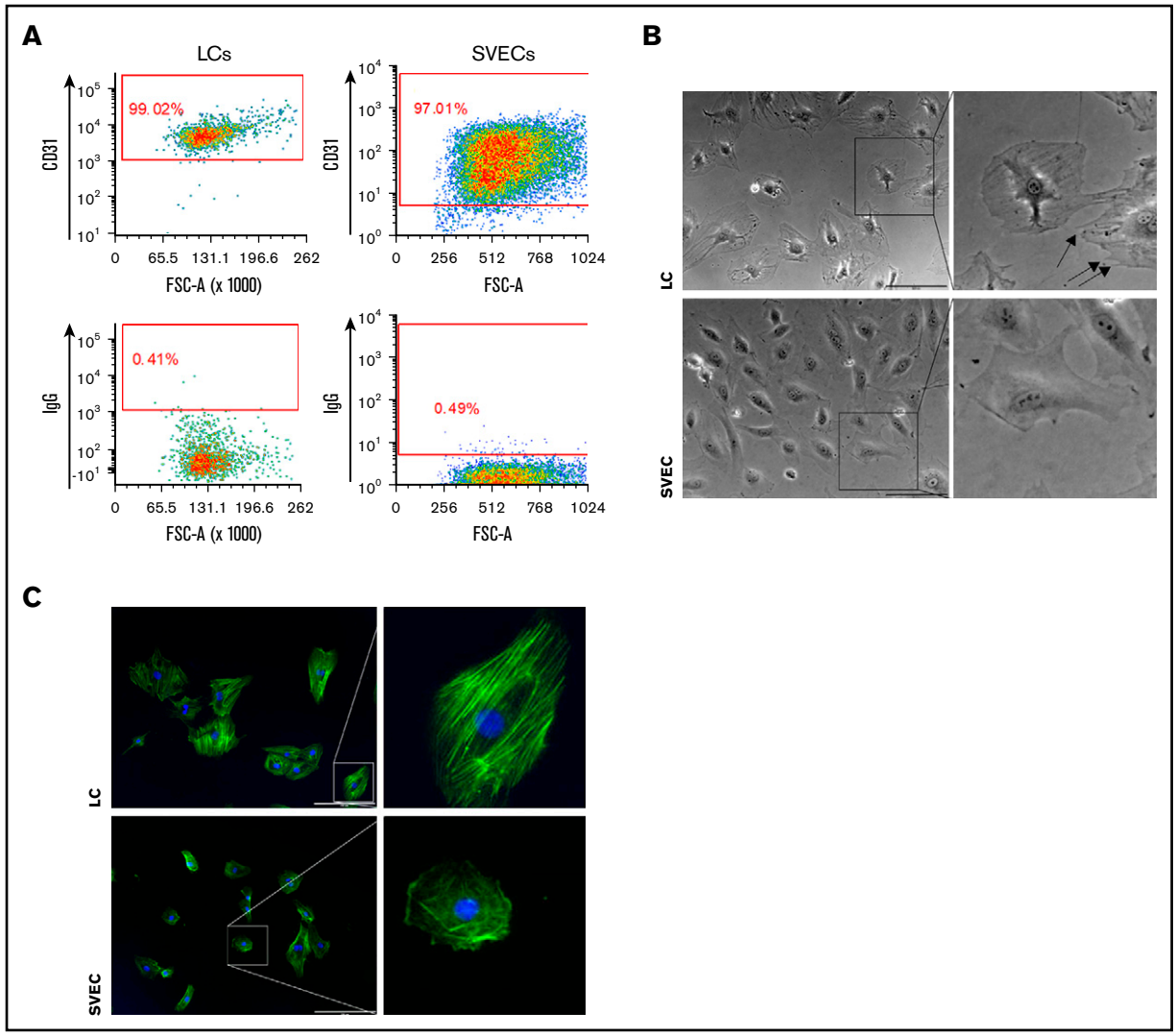

Figure 3. Morphological difference between cultured LCs and SVECs. (A) Representative FACS profiles of CD31 immunostaining of LC (left) or SVEC (right) monolayers cultured in vitro. Profiles of isotype controls are at the bottom of each panel. (B) Representative bright field photomicrographs (original magnification ×100) of LCs (top, left) and SVECs (bottom, left). (Right) Magnified images of representative cells in the square in left panels. Scale bars, 200 μm. Arrows indicate spike-like membrane protrusions in LCs. Both cell types in the paired images were simultaneously sorted and cultured in parallel. The images were captured with cells no later after passage 2 and represent 8 independent experiments from 5 donors. (C) Fluorescent microscopic images of actin filaments detected by phalloidin probes (original magnification ×100) in LCs (top, left) and SVECs (bottom, left). (Right) Magnified images of representative cells in the square in the left panels. Both cell types were cultured on the same surface under unstimulated condition. Green, actin; blue, DAPI. Scale bars, 200 μm.

(ScienCell) and incubated at 37°C and 5% CO_2. Nonadherent cells were removed on day 2. Half the medium was changed twice a week. Once a monolayer of cells formed, they were serially subcultured at a ratio of 1:4 in larger wells/dishes coated with collagen.[20]

Cocultures and CFU assays

Normal SVECs (passage 4-5) were collected after reaching 80% confluence and replated in collagen-coated 6-well plates at 7×10^5 cells/well and irradiated with 20 Gy. Three thousand normal or MF splenic $CD34^+$ cells were then seeded on the SVEC monolayers and cultured for a designated period of time in 5 mL MyeloCult H5100 (Stemcell Technologies). At the termination of the culture, cells were collected, washed, and plated in methylcellulose medium (H4230; Stemcell Technologies) supplemented with a cytokine mixture (stem cell factor [SCF], thrombopoietin, interleukin-6 [IL-6], IL-3, granulocyte colony-stimulating factor [each at 100 ng/mL], erythropoietin at 4 U/mL), according to manufacturer's instructions, and the number of hematopoietic colonies formed was enumerated after 14 days of incubation.

Results

Flow cytometric isolation of LCs and SVECs from human spleens

SVECs and LCs were identified in normal splenic tissue, using immunohistochemistry. The use of both anti- CD8α and CD34 mAbs allowed one to distinguish LCs from other SVECs. CD8α mAb staining identified LCs but not SVECs, whereas CD34 mAb staining identified SVECs but not LCs (Figure 1A). For further

Table 1. Top reduced downstream functions in normal LCs

Functions annotation	*P*, -log	Activation *z*-score
Mitogenesis	4.656	−3.692
Proliferation of vascular endothelial cells	7.526	−2.976
Cell movement of tumor cell lines	15.38	−2.748
Cell cycle progression	4.298	−2.703
Tubulation of cells	9.312	−2.481
Mitogenesis of endothelial cells	4.810	−2.330
Tubulation of endothelial cell lines	3.462	−2.153
Outgrowth of cells	3.202	−2.016
Apoptosis	14.33	−2.01
Tubulation of endothelial colony-forming cells	3.013	−2.000

IPA of LC-SVEC gene signature for top-reduced downstream functions in normal LCs compared with SVECs. *P* value (displayed as -log) indicates the significance of an association with the change of a related function. *z*-score predicts the direction of the change. Negative *z*-score indicates a decrease of a function in LCs compared with SVECs.

Table 2. Top canonical pathways in normal LCs

Canonical pathways	*P*, -log	*z*-score	Prediction	Ratio (%)
Rho GDI signaling	2.594	−1.964	Down	28/172 (16.3)
FGF signaling	3.137	−1.886	Down	18/85 (21.2)
VEGF signaling pathway	2.487	−2.000	Down	17/89 (19.1)
Chemokine signaling	3.9	−2.668	Down	17/68 (25)

IPA analysis of LC-SVEC gene signature for top-changed canonical pathways in LCs compared with SVECs. *P* value (displayed as the -log) indicates the significance of an association with the change of a related pathway. Positive or negative *z*-score predicts activation or inhibition (as indicated in the prediction column) of a pathway in LCs compared with SVECs. The ratio indicates the percentage of the genes in a given pathway in the LC-SVEC gene signature relative to the total number of genes that make up a given pathway in the whole genome.

characterization and functional studies of these 2 cell types, we established a strategy to isolate viable LCs and SVECs from collagenase digested splenic tissues, using mAb staining and cell sorting. After RBC lysis and $CD45^+$ cell depletion, splenic cells were stained with mAbs against CD45, CD3, CD8α, CD34, and CD31. FACS analysis revealed 2 distinct cell populations within a $CD45^-CD3^-$ gate, $CD34^+CD8\alpha^-CD31^+$ cells and $CD34^-CD8\alpha^+CD31^+$ cells, which represented SVECs and LCs, respectively (Figure 1B). Although both cell types expressed CD31, the expression by LCs was distinctly less than SVECs (Figure 1C). In addition, LCs were characterized by higher light scatter signals than SVECs (Figure 1D). The expression pattern of the macrophage mannose receptor (CD206) also distinguished LCs and SVECs (Figure 1E).

Global gene expression profile analysis of purified LCs and SVECs

Gene expression profiling was used to view the transcriptional properties of LCs and SVECs. Gene Expression Commons (GEXC) analysis was applied to determine the absolute gene expression activity (GEA) values of individual genes of interest.[21] The GEA of the purified LCs and SVECs further confirmed the lack of CD8β and CD45 expression and a high degree of expression of the endothelial markers PECAM1 (CD31) and VWF by both cell types, the expression of FHOD1 and CD8α by LCs but not SVECs, and the lack of CD34 expression by LCs (Figure 2A). The observation that genes detected by 92.3% of the probes were similarly expressed by both cell types (Figure 2B), as well as that the Pearson correlation coefficient was high (0.777; Figure 2C), indicating that LCs represent a specialized form of EC.

A list of 341 probes of LC-SVEC specific genes was created, using stringent criteria. The top differentially expressed genes by LCs and SVECs were identified (Figure 2D; supplemental Table 1). We next created a more inclusive LC-SVEC gene signature composed of 2345 probes of differentially expressed genes (Figure 2E). DAVID Functional Annotation Clustering analysis[22] (Figure 2F) and ingenuity pathway analysis (IPA) were then applied (Table 1; Table 2). The value of GEA of selected genes was determined for LCs and SVECs by GEXC analysis (Figure 2G,I). The results were then validated by quantitative reverse transcription polymerase chain reaction (RT-qPCR; Figure 2H,J). The downregulated genes in LCs compared with SVECs were enriched for genes involved in blood vessel formation, including cell proliferation, cell migration, and angiogenesis (Figure 2Fi; Table 1), as well as genes involved in intercellular and cell-extracellular matrix interactions (Figure 2Fi). Fibroblast growth factor (FGF), vascular endothelial growth factor (VEGF), and chemokine signaling pathways were each predicted by IPA to be downregulated in LCs (Table 2). In contrast, LCs were characterized by increased gene transcripts involved in endocytosis and iron transport (Figure 2Fii). Genes encoding phagocytosis markers, especially CD206 and Stabilin-1 and Stabilin-2, were highly expressed in LCs but not SVECs; neither cell type expressed macrophage markers (Figure 2G-H). Moreover, genes encoding cytoskeletal components and their upstream regulators in the Rho GTPase signaling pathway were differentially expressed by LCs and SVECs (Figure 2Fiii,I-J). *RHOU*, which encodes Wrch-1, an atypical Rho GTPase family member,[23-25] was highly expressed by LCs (GEA, 95.70%), but not SVECs (Figure 2I). Both *RHOU* and the GTPase-activating protein encoding gene, *ARHGAP8*, were among the top 20 most upregulated genes by LCs (Figure 2D). In contrast, Rho GDI signaling, which inhibits the GTPases, was predicted to be inactivated in LCs by IPA canonical pathway analysis (Table 2). These findings indicate that LCs have specialized cellular functions distinct from the rest of the SVECs, which likely reflect their proposed role as a RBC filter and scavenger.

Cellular structure, proliferative and functional properties of LCs and SVECs

Distinct cell skeleton structure of cultured LCs and SVECs. To further characterize their cellular and functional properties, purified LCs and SVECs were cultured in parallel. Each cell type was capable of forming cobblestone areas and later monolayers and continued to express CD31 during the culture period (Figure 3A). Unlike SVECs, which exhibited the typical polygonal shape of ECs, LCs appeared more polarized and spindle shaped. Prominent cable-like structures extended from the center to the long axis of LCs. Spike-like membrane protrusions formed at the poles of LCs. In contrast, the cytoplasm of SVECs exhibited a more uniform appearance (Figure 3B). We then stained the actin filaments of LCs and SVECs. SVECs were characterized by networks of fine actin filaments assembled in random directions or located along the cell edge, whereas LCs were characterized by thick actin cables aligned in parallel along the long axis (Figure 3C).

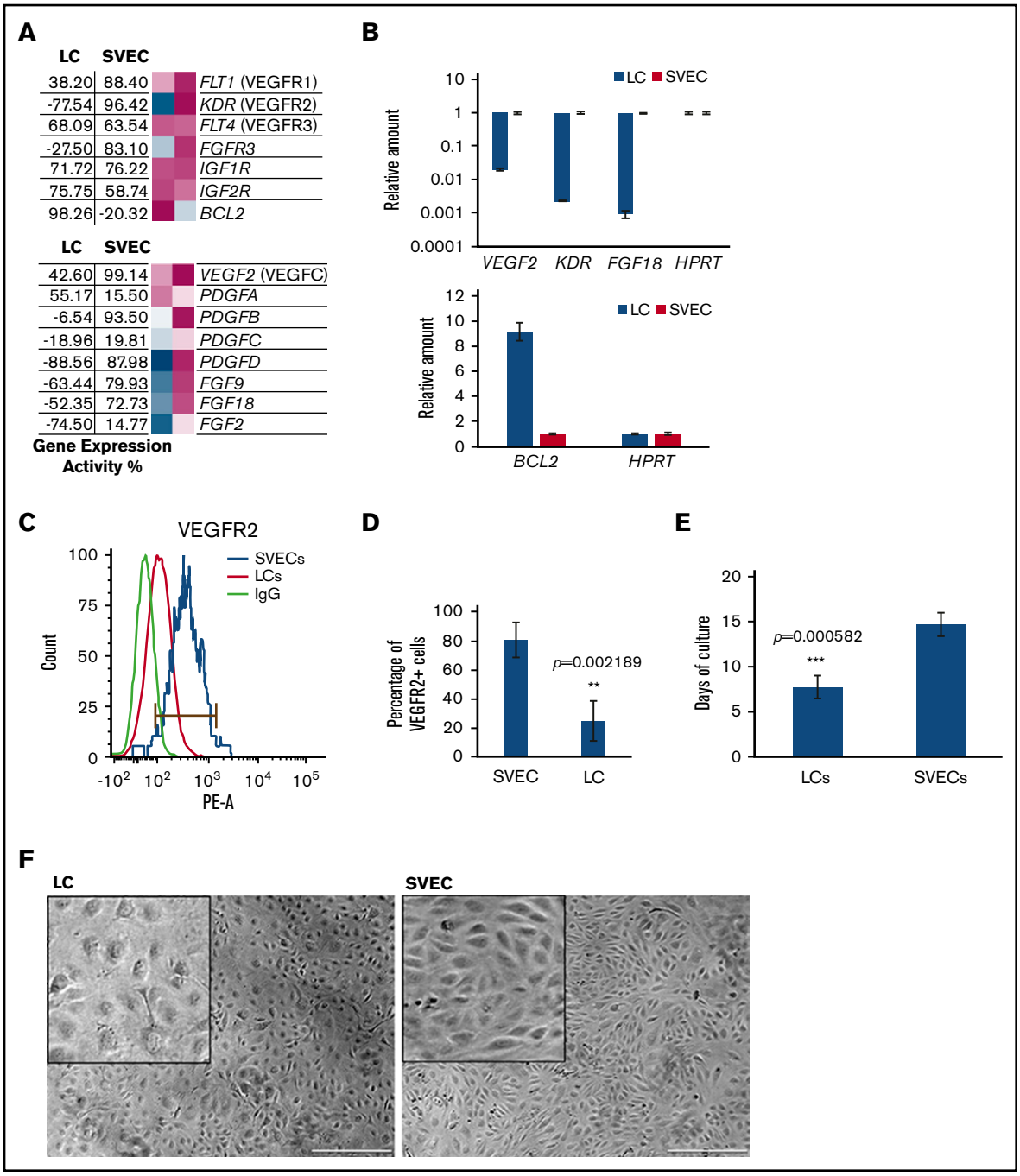

Figure 4. Characteristics of proliferation of LCs and SVECs. (A) The GEA values of selected genes encoding growth factor receptors and BCL2 (upper), and growth factors (lower), as described in Figure 2A. (B) RT-qPCR analysis of *VEGF2* (VEGF C), *KDR* (VEGFR2), *FGF18*, and *BCL2*, as described in Figure 2H. (C) Representative FACS histogram of cell surface expression of VEGFR2 by LCs and SVECs. (D) Percentage of VEGFR2 positive LCs and SVECs. Data are shown as mean ± SD, n = 3 (triplicate analyses). ***P* = .002189 by paired Student *t* test. (E) Days required to cover the entire surface of a well in 96-well plate after the initial seeding of an equal number of sorted LCs and SVECs. The result represents an average of 4 independent experiments for each line of LCs or SVECs established from a total of 5 different spleen samples. ****P* = .000582 by 2-sample Student *t* test. (F) Representative bright field photomicrographs (original magnification ×40) of LC (left) or SVEC (right) monolayers after their initial passage. Inserted squares show magnified images. Scale bars, 500 μm. Paired images of LC and SVEC cultures were captured in the same experiment performed in parallel, started with the same seeding number, and were sorted from the same spleen sample. Similar pairwise comparisons have been conducted in at least 3 independent experiments from 5 different spleen samples. IGF1R, insulin-like growth factor 1 receptor.

Reduced cell proliferative potential of LCs compared with SVECs. The global gene expression profiling indicated reduced cell proliferation and growth factor signaling activities in LCs (Figure 2Fi; Table 2). The expression of relevant genes and their products were then individually analyzed. The expression of several growth factors and receptors were reduced in LCs (Figure 4A-B).

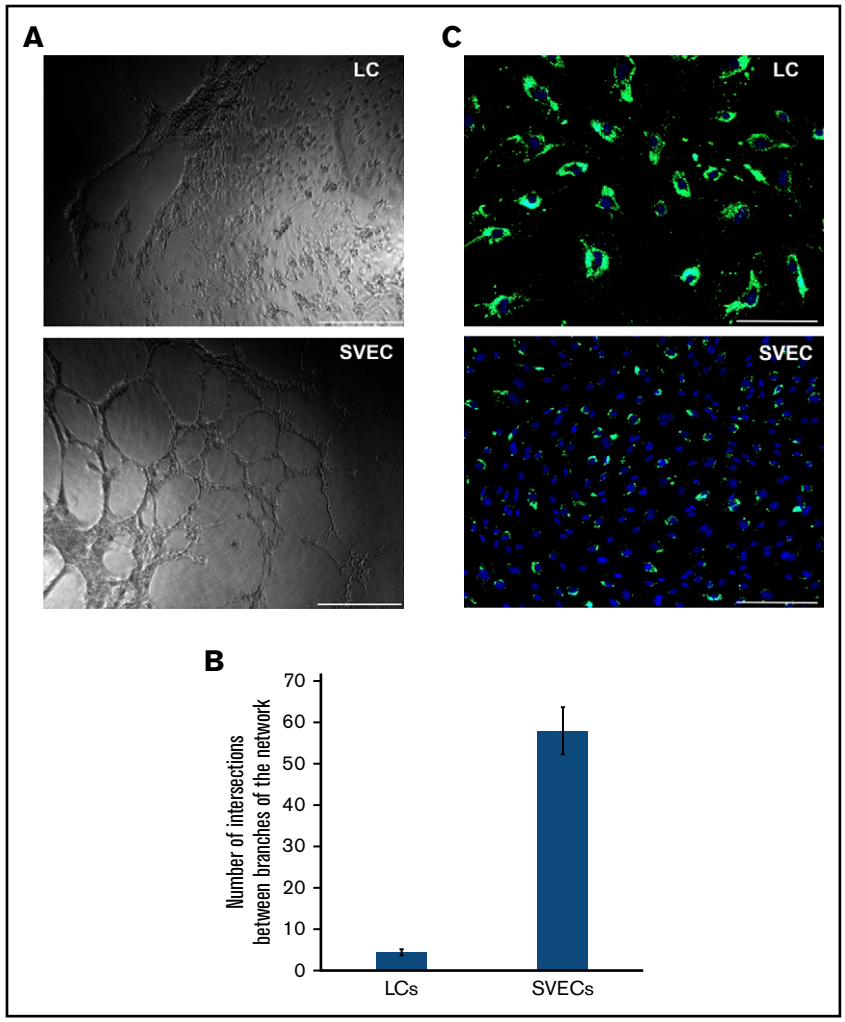

Figure 5. Functional difference between cultured LCs and SVECs. (A) Microscopic images (original magnification ×40) of in vitro tube formation by LCs (top) and SVECs (bottom) in extracellular matrix gel 5 hours after seeding. Scale bar, 500 μm. (B) The number of intersections between the branches of the tubular network formed in a single well of a 96-well plate. (C) Fluorescent microscopic images (original magnification ×100) of phagocytosis of fluorescent polystyrene microspheres by LCs (top), SVECs (bottom). Green, microspheres; blue, DAPI. Scale bar, 200 μm. Each pair of fluorescent microscopic images of LCs and SVECs was captured using the same exposure time. The images of both panels A and C are representative of experiments repeated for more 3 times with cultured cells sorted from 5 different spleen samples.

The anti-apoptosis gene *BCL2* was highly expressed in LCs (GEA, 98.26%), but not SVECs (Figure 4A-B). Notably, the endothelial marker VEGFR2 was highly expressed in SVECs (GEA, 96.42%), but not LCs (GEA, −77.54%; Figure 4A-B). FACS analyses confirmed that VEGFR2 was expressed by a smaller percentage of LCs with a lower signal intensity than SVECs (Figure 4C-D). These findings indicated that LCs have a lower proliferative potential than SVECs. We next assessed their in vitro proliferative potential. As shown in Figure 4E, SVECs required a longer interval (2-3 weeks) than LCs (1 week) in the initial culture to form a monolayer and cover the entire culture well. SVECs, but not LCs, of similar passages then proliferated more robustly for at least 6 passages, covering the same surface area with a higher density (Figure 4F). LCs, however, experienced a progressively diminished proliferative potential before reaching passage 4.

Distinct functions of in vitro cultured LCs and SVECs. To examine the functional properties of cultured LCs and SVECs, we first compared the angiogenic potential of these 2 cell types. Both cell types were able to form tubular structures (supplemental Figure 2). However, only SVECs formed networks with multiple branches (Figure 5A-B). Next, we assessed their phagocytic capacity by incubating them with fluorescent microparticles. As shown in Figure 5C, almost all LCs, but not SVECs, phagocytosed microparticles. A far greater number of intracellular fluorescent particles surrounding the nuclei were observed in LCs than SVECs. Whereas, macrophages exhibited the greatest number of fluorescent phagocytosed particles, very few particles were seen within the cytoplasm of splenic stromal cells. (supplemental Figure 1).

Expression of hematopoietic factors and adhesion molecules by normal LCs and SVECs. To better understand the potential for LCs and SVECs to elaborate factors that might affect hematopoiesis, we examined the expression of transcripts for cytokines, chemokines, adhesive molecules, and other signaling molecules that support hematopoiesis (Figure 6A). The data obtained by GEXC analysis was confirmed with real time RT-qPCR (Figure 6B). SVECs expressed higher levels of CXCL12, SCF, IL-33, JAG1, JAG2, and DLL1 transcripts compared with LCs. In particular, the GEA values of several Notch ligands by SVECs were as high as more than 90%, including DLL1 (GEA, 95.02%), JAG1 (GEA, 94.00%), and JAG2 (GEA, 99.78%; Figure 6A-B). In contrast, transcripts for IL-34, which promotes the differentiation of monocytes and macrophages, and IL-15, which promotes the differentiation of T/NK cells,[26-29] were

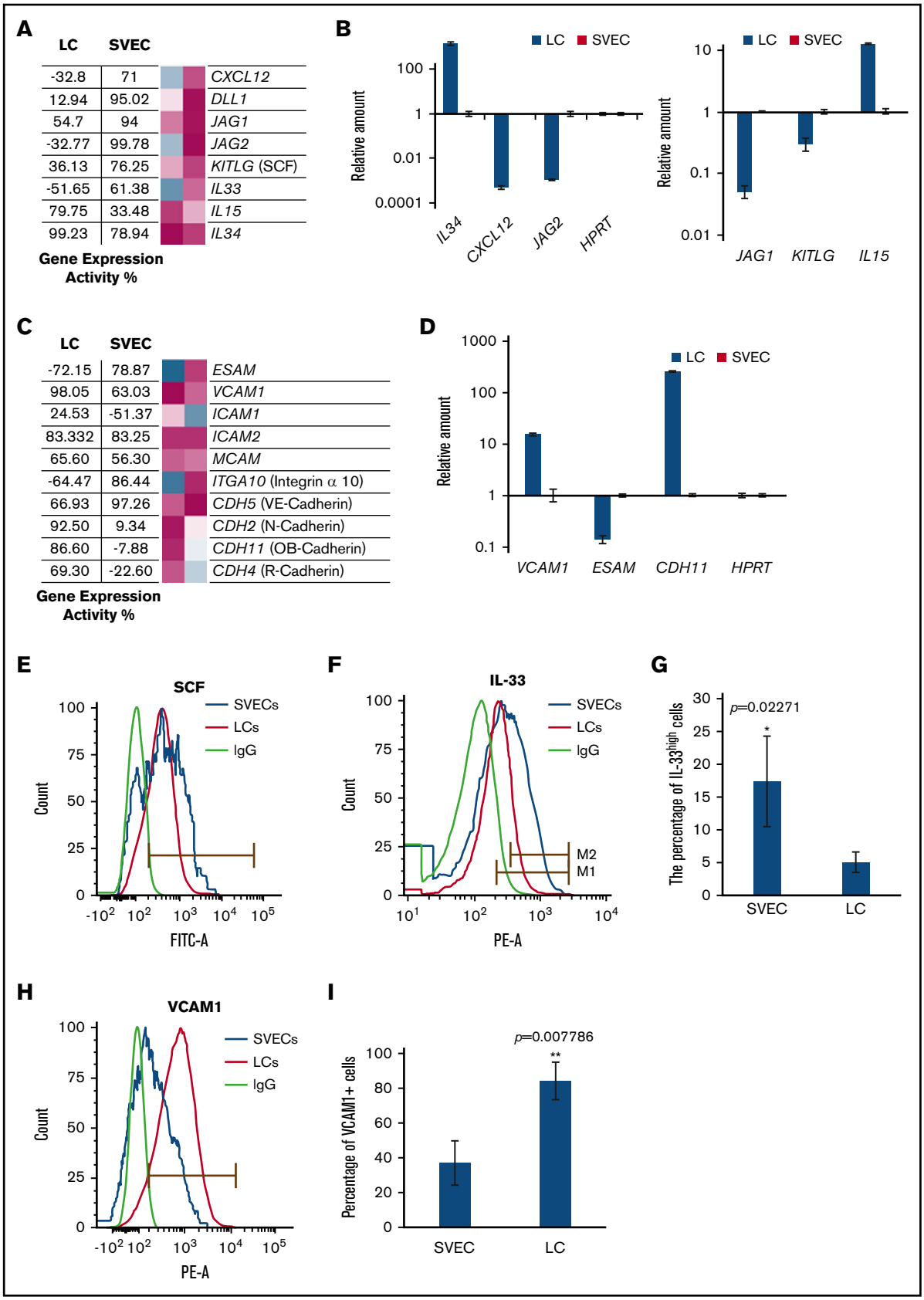

Figure 6. Hematopoietic factor and adhesion molecule production by LCs and SVECs. (A) The GEA values (as described in Figure 2A) of genes encoding factors supporting hematopoiesis. (B) RT-qPCR analysis of *IL15*, *IL34*, *KITLG* (SCF), *CXCL12*, *JAG1*, and *JAG2*, as described in Figure 2H. (C) The GEA values of genes encoding

expressed to a greater degree by LCs (GEA of IL-34, 99.23%; Figure 6A-B). In addition, LCs and SVECs had distinct expression patterns of cell adhesion molecules, particularly cadherins (Figure 6C-D). Transcripts for VCAM1 was highly expressed by LCs (GEA, 98.05%), to a greater degree than SVECs (GEA, 63.03%; Figure 6C-D). The expression of SCF, IL-33, and VCAM1 were then confirmed by mAb staining and FACS analysis. Both LCs and SVECs expressed membrane-bound SCF (Figure 6E). As shown in Figure 6F-G, a greater percentage of SVECs than LCs were IL-33^{high}. Furthermore, 90% of LCs were VCAM1^{+} compared with 40% of SVECs (Figure 6H-I).

The properties of SVECs and LCs in MF patient spleens. Immunohistochemical staining of MF spleens revealed dilated sinusoids interspersed with hematopoietic cells with a reduced density of LCs, but not SVECs, compared with normal spleens (Figure 7A). Reticulin staining showed that MF spleens were characterized by a greater degree of fibrosis (Figure 7A). Furthermore, the percentage of LCs relative to the total number of nonhematopoietic cells was decreased from an average of 50.8% in normal spleens to 8.0% in MF spleens (a reduction of 84%; $P = 3.06E-06$). In contrast, a significant decrease in the percentage of SVECs was not observed (Figure 7B-C). To determine the molecular changes underlying the characteristics of LCs and SVECs in MF spleens, the gene expression profiles of MF SVECs or LCs were compared with their normal counterparts. Gene signatures composed of, respectively, 2301 and 6348 probes of differentially expressed genes that distinguished MF from normal SVECs and LCs were created following the same criteria (Figure 7D). A greater percentage of the genes were upregulated (57.03%) than downregulated (42.85%) in MF SVECs, whereas a greater percentage of genes were downregulated (65.52%) than upregulated (34.48%) in MF LCs (Figure 7D). MF LCs were characterized by downregulation of genes involved in mitochondrial ATP biosynthesis, mRNA processing, and protein synthesis and catabolism (Figure 7E). IPA canonical pathway analysis further indicated that the changes in MF LC gene expression were significantly associated with oxidative phosphorylation ($P = 7.49E-6$), mitochondrial dysfunction ($P = 1.83E-6$), and ubiquitination ($P = 7.26E-6$; Table 3). A network was revealed by IPA analysis composed primarily of downregulated genes of ATP synthases, ribosomal proteins, nicotinamide adenine dinucleotide hydride ubiquinone oxidoreductase subunits, and cytochrome C oxidase subunits (Figure 7F). The genes in this network are positively regulated by the insulin-like growth factor 1 receptor and negatively regulated by RICTOR, a subunit of the mTOR complex 2, which is associated with autophagy.[30,31] RICTOR was also predicted to be the top activated upstream regulator ($z = 8.578$; $P = 7.11E-14$) in MF LCs by IPA upstream regulation analysis in MF LCs, whereas insulin-like growth factor 1 receptor was predicted to be an inhibited upstream regulator ($z = -2.032$; $P = .0456$). Moreover, IPA disease or function analysis predicted that apoptosis, cell death and necrosis pathways were increased in MF LCs, but not SVECs (Figure 7G), whereas the gene expression of BCL-2 was greatly decreased in MF LCs compared with normal LCs (Figure 7J). MF LCs were also characterized by further increased expression of genes for the scavenger receptor, Stabilin-1 (*STAB1*; Figure 7J). Transcripts of interleukin 1 receptor type 1, which are increased in the plasma of patients with MF,[32] were highly expressed in normal LCs, but not SVECs, and were expressed to an even greater degree by MF LCs (Figure 7J), with a GEA value of 99.99% (data not shown).

MF SVECs were shown by IPA downstream functional analysis to be more active in cell growth and migration compared with normal SVECs, whereas MF LCs did not show any changes in these categories (Figure 7H). DAVID Functional Annotation Analysis revealed that the genes upregulated in MF SVECs were enriched for the annotation "type I IFN signaling pathway" ($P = 4.50E-03$) and "G/M transition of the mitotic cell cycle" ($P = 9.90E-04$; Figure 7I). We then performed IPA analysis to predict the direction of activation of enriched canonical pathways. Interferon (IFN) signaling was predicted to be activated ($P = 1.61E-02$; $z = 2.12$; Table 4; supplemental Table 2), whereas the cell cycle G1/S checkpoint regulation was diminished ($P = 6.34E-03$; $z = -1.941$) in MF SVECs (Table 4). As shown in Figure 7J, the expression of the G1 phase CDK inhibitor p57 gene was downregulated, whereas angiopoietin-2, VEGF receptor 1 and 2, and BCL-2 gene expression were each upregulated in MF compared with normal SVECs (Figure 7J). Several factors that support hematopoiesis, including the Notch ligands DLL1 and DLL4, SCF, IL-33, and IL-15 were each expressed at a higher level by MF than normal SVECs (Figure 7J). In particular, the GEA value of IL-33 increased from 61.38% in normal SVEC to 94.47% in MF SVECs (data not shown).

To examine whether SVECs were capable of supporting hematopoiesis, MF and normal splenic CD34^{+} cells were cocultured with monolayers of normal SVECs, and the cultures were then assayed for hematopoietic progenitor cells. MF, but not normal CD34^{+} cells, generated numerous numbers of assayable progenitor cells after 4 and 6 days of coculture (Figure 7K). Normal CD34^{+} cells were also cocultured with normal or MF SVECs. Unfortunately, only 1 line of MF SVECs from a single donor was available for this assay. This line of MF SVECs supported the generation of greater numbers of assayable hematopoietic progenitor cells than normal SVECs (Figure 7L). Furthermore, a greater number of colonies was generated from MF splenic CD34^{+} cells after a long-term culture with MF stromal cells than with normal bone marrow (BM) mesenchymal stem cells (MSCs), although the culture with BM MSCs gave rise to primarily large GEMM (granulocyte, erythrocyte, monocyte, megakaryocyte) colonies (supplemental Figure 3). Long-term culture with SVECs were not performed, for SVEC layers could not be maintained in the coculture for more than 5 weeks. We were unable to establish cocultures with LC monolayers, for LCs were unable to survive under myeloid culture medium conditions without the addition of endothelial growth factor supplements.

Figure 6. (continued) adhesion molecules. (D) RT-qPCR analysis of *VCAM1*, *ESAM*, and *CDH11* (OB-cadherin), as described in Figure 2H. (E) Representative FACS histogram of SCF cell surface expression by LCs and SVECS. (F) Representative FACS histogram of intracellular IL-33 in fixed LCs and SVECS. Gate M1: IL-33^{+} based on IgG. Gate M2: IL-33^{high}. (G) The percentage of IL-33^{high} cells (Gate M2) relative to total LCs and SVECs. Data are shown as mean ± SD, n = 3 (triplicate analyses). *$P = .02271$ by paired Student *t* test. (H) Representative FACS histograms of VCAM1. (I) Percentage of VCAM1^{+} cells in SVECs and LCs. Data are shown as mean ± SD, n ≥ 3. **$P = .007786$ by 2-sample Student *t* test.

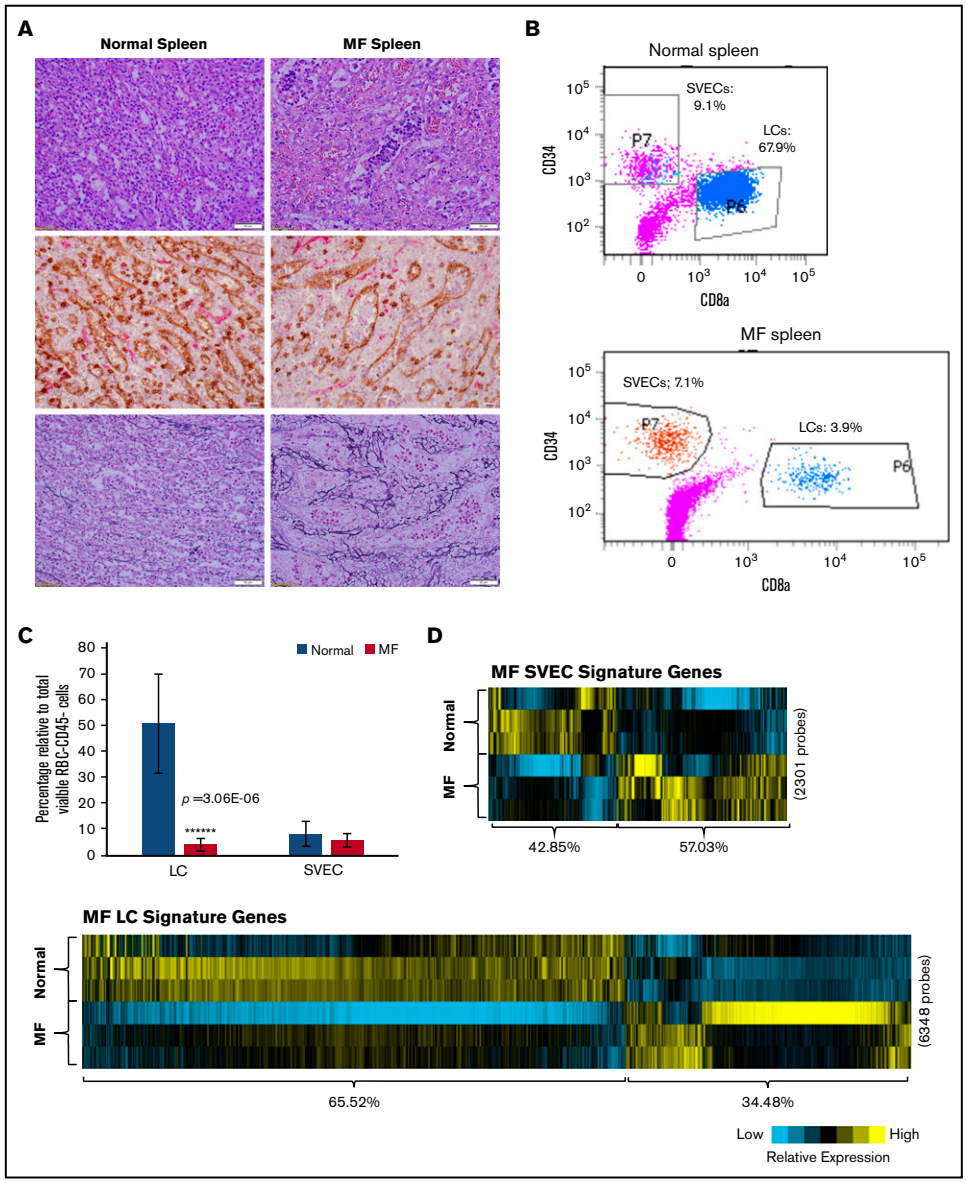

Figure 7. The properties of MF LCs and SVECs. (A, upper) Representative photomicrograph of hematoxylin and eosin staining of the red pulp of normal and MF spleens. Scale bar, 50 μm. (Middle) Matching samples stained with both anti-CD8α (brown) and anti-CD34 (magenta) antibodies. LCs are stained brown, SVECs are stained magenta. Scale bar, 20 μm. (Bottom) Reticulin staining of the matching samples as earlier. Scale bar, 50 μm. Pictures of all 3 panels were taken at 400× original magnification. (B) Representative FACS profiles of normal or MF nonhematopoietic cell fraction from collagenase digested nonsuspensive part of spleen tissues, which are $CD45^{-}CD3^{-}$ and RBC-free. The percentages of LCs and SVECs are indicated in the profiles. (C) Percentage of normal or MF LCs and SVECs relative to total viable $CD45^{-}CD3^{-}$, RBC-free, nonhematopoietic splenic cells as in (B). Data are shown as mean ± SD, n > 3. ******P = 3.06E-06 by 2-sample Student t test. The result represents an average of 4 independent experiments with spleens from 4 patients with MF and 6 normal individuals. (D) The heat map of relative gene expression intensity for MF SVEC or LC gene signature. (Upper) MF SVECs; (lower) MF LCs. (E) DAVID Functional Annotation Clustering analysis of MF LC gene signature for downregulated genes in MF compared with normal LCs. (F) A network of energy production, nucleic acid metabolism, and small molecule biochemistry by IPA analysis of genes differentially expressed in MF compared with normal LCs. Network score, 27; focus molecules, 34; green, gene expression downregulated in MF LCs; red: gene expression upregulated in MF LCs; dotted arrow lines, direction of regulation. (G) z-scores of apoptosis, cell death, and necrosis by IPA disease or function analysis for MF LCs and SVECs compared with their normal counterparts. Activation z-score ≥2 predicts the increase of a function; ≤−2 predicts the decrease of a function. P value indicates the significance of an association with the change of a related function. (H) z-scores of cell movement, migration, and outgrowth of cells by IPA disease or function analysis for MF LCs and SVECs compared with their normal counterparts. MF LCs did not have any significant change with a qualified P value in these annotations. (I) DAVID Functional Annotation Clustering analysis of upregulated genes in MF SVECs compared with normal SVECs. (J) The heat map of relative average expression intensity for selected genes by normal or MF SVECs and LCs. (K) The number of colony forming units (CFUs) formed in the colony-forming assay after the cocultures of 3000 normal or MF splenic $CD34^{+}$ cells with normal SVEC cell layers for 4 days (left graph) or 6 days (right graph). $CD34^{+}$ cells of 1 MF and 2 normal spleens obtained from different individual donors were cocultured in parallel with each of the 2 lines of normal SVECs (#1 and #2). Each $CD34^{+}$ cell coculture was plotted individually (blue, normal; red, MF). (L) The number of assayable CFUs after coculture of 3000 normal splenic $CD34^{+}$ cells from 3 different donors each with 2 lines of normal or 1 line of MF SVECs for 4 to 6 days. IL1R1, interleukin 1 receptor type 1; NADH, nicotinamide adenine dinucleotide hydride.

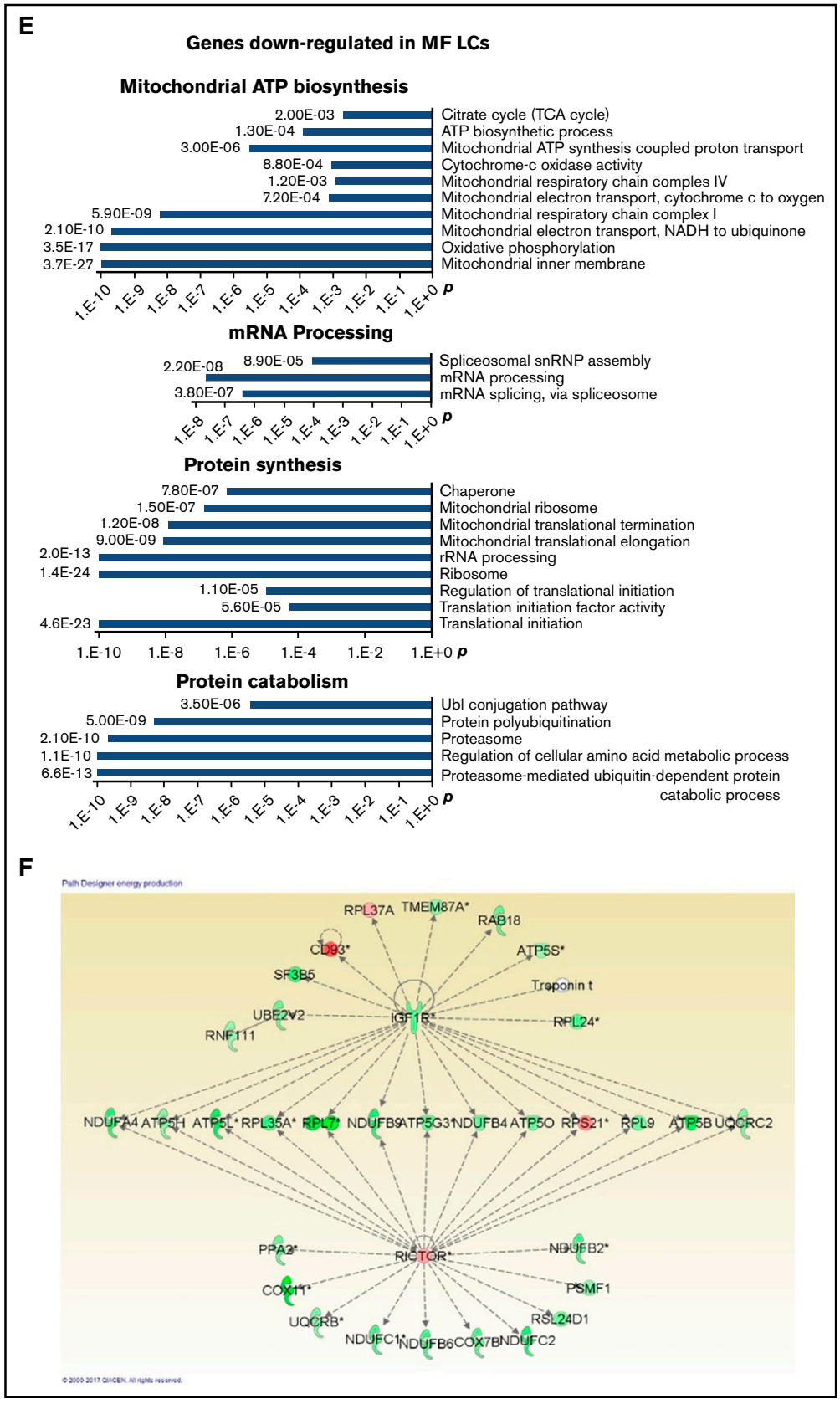

Figure 7. (Continued).

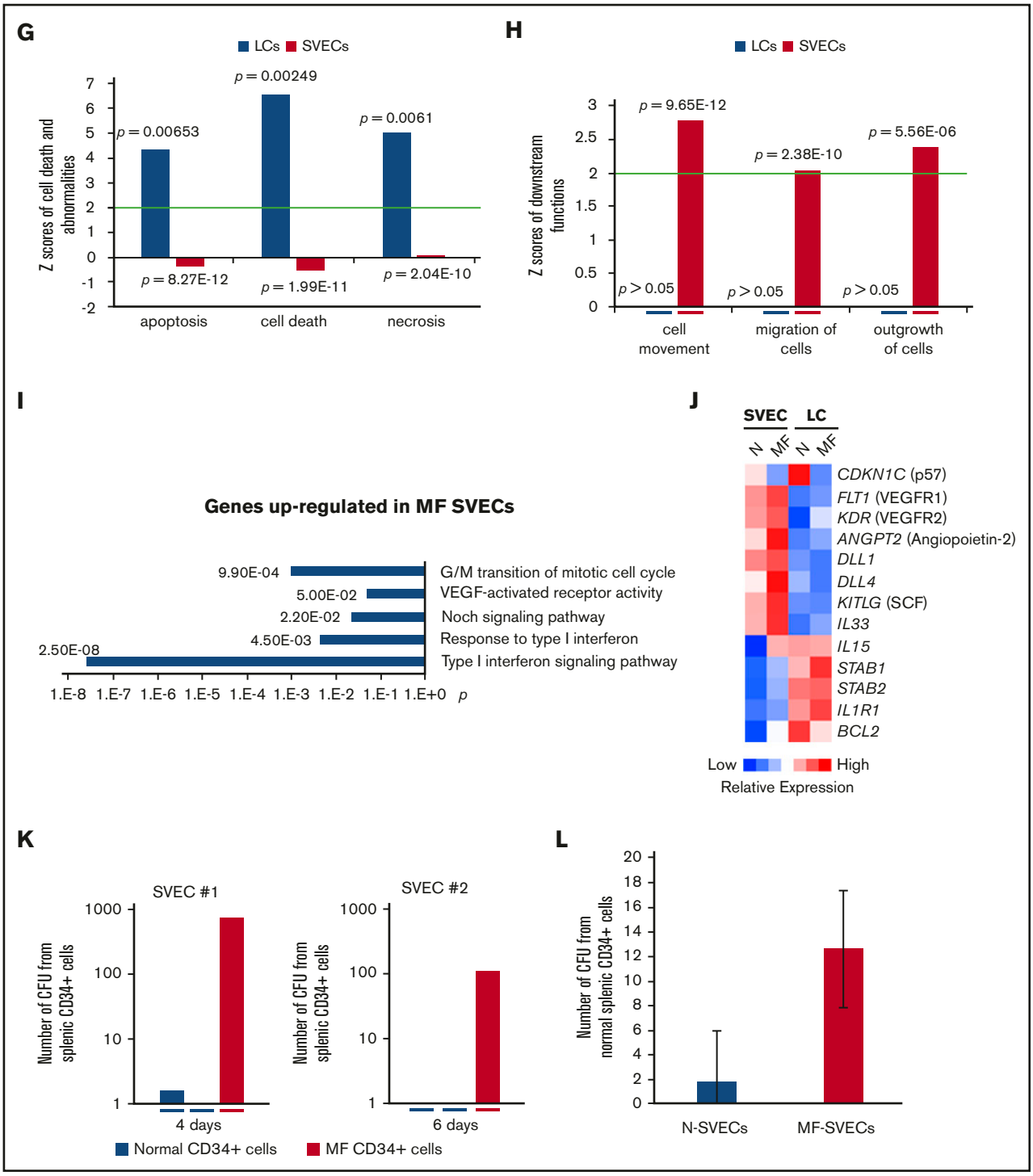

Figure 7. (Continued).

Discussion

We provide evidence that LCs represent a specialized form of EC with molecular characteristics that support their long assumed role as filters and scavengers of cellular debris. LCs possess a unique gene expression pattern encoding cytoskeleton organizers and upstream regulators in the GTPase signaling pathway. We observed that thick actin cables were aligned in parallel along the axis of cultured LCs, but not SVECs in resting state, which indicates the unique cytoskeleton likely provides the rigidity of the sinusoidal slits needed to serve as RBC filters, and the resistance to sustain the shear force generated during the filtration.[1,5]

Table 3. Top diseases or functions in MF LCs

Canonical pathways	*P*, -log	% (ratio)
Oxidative phosphorylation	5.125	50 (41/82)
Mitochondrial dysfunction	5.738	45.7 (63/138)
Ubiquitination pathway	5.139	40.7 (88/216)

IPA analysis of MF LC gene signature for diseases or functions in MF compared with normal LCs. See Table 1 for more information. No *z*-score is available for the listed pathways.

The spleen sustains hematopoiesis during fetal development.[33] As a secondary lymphoid organ, the adult spleen supports the proliferation and differentiation of phagocytic and antigen-presenting cells in response to inflammation from precursors traveling through circulation.[27,34-37] Very limited numbers of hematopoietic stem cells/progenitor cells (HSC/PCs) have been detected in adult normal human spleens.[38] During stressful conditions (chronic hemolytic anemias and hemoglobinopathies), EMH can develop. Splenic EMH occurs in the red pulp,[39] which is largely a vascular microenvironment. Studies have shown that splenic ECs play an important role during stress induced murine EMH by producing SCF and CXCL12.[40] However, murine spleens are structurally distinct from human spleens.[4] The endothelium of various sites along the vascular tree are highly heterogeneous in phenotype and function.[41,42] At this time, the knowledge of the individual contributions of LCs and SVECs to the development of EMH within human spleens is limited. In this study, we showed that LCs and SVECs express both overlapping and distinct gene products including CXCL12, SCF, IL-33, VCAM1, and Notch ligands (DLL1, DLL4, and JAG1, 2) that can mobilize, attract, retain, and promote the proliferation of HSC/PCs. Many of these factors are expressed at higher levels by SVECs than LCs. LCs and SVECs also express different cell adhesion molecules. Although VCAM1 is known to be constitutively expressed at moderate levels by resting ECs, it was much more highly expressed by both normal and MF LCs. VCAM1$^+$ macrophages have been shown to be essential for the development of EMH in mice by promoting the retention of hematopoietic cells.[43] We speculate that increased expression of VCAM1 by LCs compared with SVECs might contribute to the retention of HSC/PCs within the spleen and help initiate EMH during the early stage of MF.

The development of EMH in MF is likely a result of the constitutive mobilization of HSC/PCs. These mobilized cells likely localize in the spleen because of the high expression of chemokines and adhesion molecules such as CXCL12 and possibly VCAM1, allowing establishment of EMH in response to the hematopoietic growth promoting factors produced by both SVECs and LCs. In support of this hypothesis, we have previously reported that in the MF spleen, CXCL12 remains structurally intact and fully capable of acting as a chemoattractant compared with CXCL12 in the peripheral blood, which has been degraded and has fewer chemoattractant properties.[44] In addition, our laboratory has also reported the presence of greater numbers of malignant stem cells in the spleen compared with the peripheral blood of patients with MF.[16]

Splenic endothelial cells express many hematopoietic factors, which may be insufficient to maintain the normal hematopoietic progenitor potential. MF hematopoietic progenitors, in contrast, are more sensitive to hematopoietic growth factors and microenvironmental cues because of the characteristic driver mutations and the subsequent activation of the JAK/STAT pathway.[45] This increased sensitivity likely accounts for the generation of greater numbers of MF than normal progenitors when cocultured with SVECs. The gene expression profile of MF SVECs compared with normal SVECs was characterized by upregulation of angiopoietin-2, SCF, the Notch ligands, IL-15, and IL-33. IL-33, in particular, has been considered to play a possible role in myeloproliferative neoplasm biogenesis.[46,47] The circulation level of IL-15 has also been reported to be increased in the patients with MF.[32] An MF SVEC cell line promoted the generation of greater numbers of hematopoietic progenitor cells from normal splenic CD34$^+$ cells than normal SVEC lines. In addition, the long-term coculture of MF splenic CD34$^+$ cells with MF splenic stromal cell layers supported the generation of greater number of total colonies than similar cultures with normal BM MSC-derived cell layers. Cultures with BM MSCs layer, however, led to the generation of a higher proportion of primitive CFU-GEMM colonies. MF splenic vessel lining cells and stromal cells each provide a favorable microenvironment that likely accounts for the development of EMH in MF spleens.

The levels of IFN-α have been reported to be increased in the plasma of patients with MF.[32] We found that MF SVECs were characterized by the activation of the IFN signaling and cell cycle progression pathways. Previously, IFN has been shown to promote EC proliferation in vitro and in vivo.[48,49] The activation of interferon signaling within MF SVECs likely occurs in response to the MF inflammatory milieu that leads to further SVEC proliferation. Such proliferation of SVECs likely culminates in the increased density of capillaries observed in MF spleens.[17]

Unlike MF SVECs, LCs from MF spleens were characterized by significant mitochondrial dysfunction, decreased ATP biosynthesis, protein synthesis and catabolism, and cell death. It is possible that the elevated cellular stress associated with excessive RBC filtration and phagocytosis in MF spleens might led to this gene expression pattern. LCs have a reduced proliferative potential and are less able to participate in tube formation in vitro. These properties together account for the relatively diminished sinusoidal density observed in MF spleens.

Table 4. Top canonical pathways in MF SVECs

Canonical pathways	*P*	*z*-score	Prediction	% (ratio)
Interferon signaling	.016	2.121	Activated	22.2 (8/36)
Cell cycle G1/S checkpoint regulation	.00634	−1.941	Inactivated	25.4 (16/63)

IPA analysis of MF SVEC gene signature for canonical pathways in MF compared with normal SVECs. See Table 2 for more information.

Acknowledgments

The authors thank the Flow Cytometry Shared Resource Facility at Icahn School of Medicine at Mount Sinai, Wu He and Xuqiang Qiao for excellent assistance with cell sorting service, and Sheryl Tripp (University of Utah) for performing an excellent double IHC staining.

This study was funded by grants from the National Institutes of Health, National Cancer Institute (1P01CA108671) (R.H.).

Authorship

Contribution: J.Q. conceived and designed experiments, collected, analyzed, and interpreted data, and wrote the manuscript; M.E.S. performed the immunohistochemical staining; C.S.H. and Y.L. processed splenic tissue; X.W. processed splenic tissue and critically read the manuscript; and R.H. conceived the experiments, interpreted data, and participated in writing the manuscript.

Conflict-of-interest disclosure: The authors declare no competing financial interests.

Correspondence: Ronald Hoffman, Division of Hematology/Medical Oncology, Department of Medicine, Tisch Cancer Institute, Icahn School of Medicine at Mount Sinai, 1 Gustave L. Levy Place, Box 1079, New York, NY 10029; e-mail: ronald.hoffman@mssm.edu.

Reference

1. Steiniger B, Barth P. Microanatomy and function of the spleen. *Adv Anat Embryol Cell Biol*. 2000;151:III-IX.
2. Chadburn A. The spleen: anatomy and anatomical function. *Semin Hematol*. 2000;37(1 suppl 1):13-21.
3. Brozman M, Jakubovský J. The red pulp of the human spleen. Structural basis of blood filtration. *Z Mikrosk Anat Forsch*. 1989;103(2):316-328.
4. Mebius RE, Kraal G. Structure and function of the spleen. *Nat Rev Immunol*. 2005;5(8):606-616.
5. Drenckhahn D, Wagner J. Stress fibers in the splenic sinus endothelium in situ: molecular structure, relationship to the extracellular matrix, and contractility. *J Cell Biol*. 1986;102(5):1738-1747.
6. Pusztaszeri MP, Seelentag W, Bosman FT. Immunohistochemical expression of endothelial markers CD31, CD34, von Willebrand factor, and Fli-1 in normal human tissues. *J Histochem Cytochem*. 2006;54(4):385-395.
7. Ogembo JG, Milner DA Jr, Mansfield KG, et al. SIRPα/CD172a and FHOD1 are unique markers of littoral cells, a recently evolved major cell population of red pulp of human spleen. *J Immunol*. 2012;188(9):4496-4505.
8. Gardberg M, Kaipio K, Lehtinen L, et al. FHOD1, a formin upregulated in epithelial-mesenchymal transition, participates in cancer cell migration and invasion. *PLoS One*. 2013;8(9):e74923.
9. Barnhart MI, Lusher JM. The human spleen as revealed by scanning electron microscopy. *Am J Hematol*. 1976;1(2):243-264.
10. Fujita T, Kashimura M, Adachi K. Scanning electron microscopy (SEM) studies of the spleen–normal and pathological. *Scan Electron Microsc*. 1982;(Pt 1):435-444.
11. Buckley PJ, Dickson SA, Walker WS. Human splenic sinusoidal lining cells express antigens associated with monocytes, macrophages, endothelial cells, and T lymphocytes. *J Immunol*. 1985;134(4):2310-2315.
12. Stuart AE, Warford A. Staining of human splenic sinusoids and demonstration of unusual banded structures by monoclonal antisera. *J Clin Pathol*. 1983;36(10):1176-1180.
13. Barosi G, Hoffman R. Idiopathic myelofibrosis. *Semin Hematol*. 2005;42(4):248-258.
14. Mesa RA, Barosi G, Cervantes F, Reilly JT, Tefferi A. Myelofibrosis with myeloid metaplasia: disease overview and non-transplant treatment options. *Best Pract Res Clin Haematol*. 2006;19(3):495-517.
15. Rondelli D, Barosi G, Bacigalupo A, et al; Myeloproliferative Diseases-Research Consortium. Allogeneic hematopoietic stem-cell transplantation with reduced-intensity conditioning in intermediate- or high-risk patients with myelofibrosis with myeloid metaplasia. *Blood*. 2005;105(10):4115-4119.
16. Wang X, Prakash S, Lu M, et al. Spleens of myelofibrosis patients contain malignant hematopoietic stem cells. *J Clin Invest*. 2012;122(11):3888-3899.
17. Barosi G, Rosti V, Massa M, et al. Spleen neoangiogenesis in patients with myelofibrosis with myeloid metaplasia. *Br J Haematol*. 2004;124(5):618-625.
18. de Hoon MJ, Imoto S, Nolan J, Miyano S. Open source clustering software. *Bioinformatics*. 2004;20(9):1453-1454.
19. Saldanha AJ. Java Treeview–extensible visualization of microarray data. *Bioinformatics*. 2004;20(17):3246-3248.
20. Colombo E, Calcaterra F, Cappelletti M, Mavilio D, Della Bella S. Comparison of fibronectin and collagen in supporting the isolation and expansion of endothelial progenitor cells from human adult peripheral blood. *PLoS One*. 2013;8(6):e66734.
21. Seita J, Sahoo D, Rossi DJ, et al. Gene Expression Commons: an open platform for absolute gene expression profiling. *PLoS One*. 2012;7(7):e40321.
22. Huang W, Sherman BT, Lempicki RA. Bioinformatics enrichment tools: paths toward the comprehensive functional analysis of large gene lists. *Nucleic Acids Res*. 2009;37(1):1-13.
23. Tao W, Pennica D, Xu L, Kalejta RF, Levine AJ. Wrch-1, a novel member of the Rho gene family that is regulated by Wnt-1. *Genes Dev*. 2001;15(14):1796-1807.
24. Fort P, Guémar L, Vignal E, et al. Activity of the RhoU/Wrch1 GTPase is critical for cranial neural crest cell migration. *Dev Biol*. 2011;350(2):451-463.
25. Shutes A, Berzat AC, Cox AD, Der CJ. Atypical mechanism of regulation of the Wrch-1 Rho family small GTPase. *Curr Biol*. 2004;14(22):2052-2056.
26. Mrózek E, Anderson P, Caligiuri MA. Role of interleukin-15 in the development of human CD56+ natural killer cells from CD34+ hematopoietic progenitor cells. *Blood*. 1996;87(7):2632-2640.

27. Briard D, Brouty-Boyé D, Azzarone B, Jasmin C. Fibroblasts from human spleen regulate NK cell differentiation from blood CD34(+) progenitors via cell surface IL-15. *J Immunol*. 2002;168(9):4326-4332.

28. Waldmann TA. Interleukin-15 in the treatment of cancer. *Expert Rev Clin Immunol*. 2014;10(12):1689-1701.

29. Wei S, Nandi S, Chitu V, et al. Functional overlap but differential expression of CSF-1 and IL-34 in their CSF-1 receptor-mediated regulation of myeloid cells. *J Leukoc Biol*. 2010;88(3):495-505.

30. Yang Z, Klionsky DJ. Mammalian autophagy: core molecular machinery and signaling regulation. *Curr Opin Cell Biol*. 2010;22(2):124-131.

31. Kim YC, Guan KL. mTOR: a pharmacologic target for autophagy regulation. *J Clin Invest*. 2015;125(1):25-32.

32. Tefferi A, Vaidya R, Caramazza D, Finke C, Lasho T, Pardanani A. Circulating interleukin (IL)-8, IL-2R, IL-12, and IL-15 levels are independently prognostic in primary myelofibrosis: a comprehensive cytokine profiling study. *J Clin Oncol*. 2011;29(10):1356-1363.

33. Tavian M, Péault B. Embryonic development of the human hematopoietic system. *Int J Dev Biol*. 2005;49(2-3):243-250.

34. Kim CH. Homeostatic and pathogenic extramedullary hematopoiesis. *J Blood Med*. 2010;1:13-19.

35. O'Neill HC, Griffiths KL, Periasamy P, et al. Spleen stroma maintains progenitors and supports long-term hematopoiesis. *Curr Stem Cell Res Ther*. 2014;9(4):354-363.

36. Liu K, Victora GD, Schwickert TA, et al. In vivo analysis of dendritic cell development and homeostasis. *Science*. 2009;324(5925):392-397.

37. Briard D, Azzarone B, Brouty-Boyé D. Importance of stromal determinants in the generation of dendritic and natural killer cells in the human spleen. *Clin Exp Immunol*. 2005;140(2):265-273.

38. Dor FJ, Ramirez ML, Parmar K, et al. Primitive hematopoietic cell populations reside in the spleen: Studies in the pig, baboon, and human. *Exp Hematol*. 2006;34(11):1573-1582.

39. Tavassoli M, Weiss L. An electron microscopic study of spleen in myelofibrosis with myeloid metaplasia. *Blood*. 1973;42(2):267-279.

40. Inra CN, Zhou BO, Acar M, et al. A perisinusoidal niche for extramedullary haematopoiesis in the spleen. *Nature*. 2015;527(7579):466-471.

41. Nolan DJ, Ginsberg M, Israely E, et al. Molecular signatures of tissue-specific microvascular endothelial cell heterogeneity in organ maintenance and regeneration. *Dev Cell*. 2013;26(2):204-219.

42. Aird WC. Endothelial cell heterogeneity. *Cold Spring Harb Perspect Med*. 2012;2(1):a006429.

43. Dutta P, Hoyer FF, Grigoryeva LS, et al. Macrophages retain hematopoietic stem cells in the spleen via VCAM-1. *J Exp Med*. 2015;212(4):497-512.

44. Wang X, Cho SY, Hu CS, Chen D, Roboz J, Hoffman R. C-X-C motif chemokine 12 influences the development of extramedullary hematopoiesis in the spleens of myelofibrosis patients. *Exp Hematol*. 2015;43(2):100-109.

45. Rampal R, Al-Shahrour F, Abdel-Wahab O, et al. Integrated genomic analysis illustrates the central role of JAK-STAT pathway activation in myeloproliferative neoplasm pathogenesis. *Blood*. 2014;123(22):e123-e133.

46. Kim J, Kim W, Le HT, et al. IL-33-induced hematopoietic stem and progenitor cell mobilization depends upon CCR2. *J Immunol*. 2014;193(7):3792-3802.

47. Mager LF, Riether C, Schürch CM, et al. IL-33 signaling contributes to the pathogenesis of myeloproliferative neoplasms. *J Clin Invest*. 2015;125(7):2579-2591.

48. Gomez D, Reich NC. Stimulation of primary human endothelial cell proliferation by IFN. *J Immunol*. 2003;170(11):5373-5381.

49. Prendergast AM, Kuck A, van Essen M, Haas S, Blaszkiewicz S, Essers MA. IFNα-mediated remodeling of endothelial cells in the bone marrow niche. *Haematologica*. 2017;102(3):445-453.